

# Letters

## A 3.2-kW 13.56-MHz SiC Passive Rectifier With 94.0% Efficiency Using Commutation Capacitor

Mohammad Bani Shamsheh, Itsuo Yuzurihara, and Atsuo Kawamura, *Fellow, IEEE*

**Abstract**—This letter presents a high-efficiency and high-power passive rectifier for wireless power transfer applications. A commutation capacitor is added at the input of the rectifier to improve its performance. The output current is transformed from the discontinuous conduction mode to the continuous conduction mode. The feasibility of the circuit has been verified experimentally on a 3.2-kW prototype and a maximum efficiency of 94.0% has been achieved.

**Index Terms**—Commutation capacitor, high-efficiency rectifier, parasitic components, wireless power transmission.

### I. INTRODUCTION

ONE of the popular methods for wireless power transmission that has been under extensive scrutiny in the past few years is magnetic resonant coupling [1]–[4]. This method utilizes high-frequency power sources to transmit power between two magnetically coupled coils. The frequency is usually in the megahertz range. One particular frequency that has been used extensively, which lies in the industrial, scientific, and medical frequency band, is 13.56 MHz. To build a system with high overall efficiency, it is imperative to build an ac/dc rectifier with high efficiency at the receiving coil side.

Many researchers have tackled this problem with different approaches. A semibridgeless active rectifier in which the lower diodes are replaced with synchronous switches and controlled by a phase-shifted pulse width modulation (PWM) signal has been investigated in [5]. The system achieved 94.4% efficiency at 150 kHz frequency. In [6], a class-E resonant rectifier has been reported for low-power applications with 94.4% efficiency, at 800 kHz frequency. A cycloconverter-type rectifier has been reported in [7] operating at 20 kHz frequency and has achieved 89% efficiency at 550 W. Table I summarizes a sample of recent publications in the literature concerning high-frequency rectifiers. Refs. [5] and [6] achieved high efficiencies (both about 94.4%), but the frequency of the system is below 1 MHz. For the other papers, which incorporate frequencies of 5.56 MHz or above, Park *et al.* [8], [11], and [12] have achieved 91.5%, 90.1%, and 90.9% efficiencies, respectively.

Manuscript received February 16, 2016; accepted March 3, 2016. Date of publication March 14, 2016; date of current version May 20, 2016.

M. B. Shamsheh and A. Kawamura are with the Department of Electrical and Computer Engineering, Yokohama National University, Yokohama, Kanagawa 240-8501, Japan (e-mail: bani-husam-bk@ynu.jp; kawamura@ynu.ac.jp).

I. Yuzurihara is with the Kyosan Electric Manufacturing Co., Ltd., Yokohama, Kanagawa 230-0031, Japan (e-mail: i-yuzurihara@kyosan.co.jp).

Color versions of one or more of the figures in this paper are available online at <http://ieeexplore.ieee.org>

Digital Object Identifier 10.1109/TPEL.2016.2541683

TABLE I  
SAMPLE OF RECENT PUBLICATIONS FOR HIGH FREQUENCY  
AND HIGH EFFICIENCY RECTIFIERS

Citation	Frequency	Efficiency (%)	Description	Power
[5]	150 kHz	94.4	Semibridgeless active rectifier	1 kW
[6]	800 kHz	94.43	Class-E resonant rectifier	10 W
[7]	20 kHz	89	PWM rectifier	550 W
[8]	6.78 MHz	91.5	Full CMOS active rectifier	10 W
[9]	6.78 MHz	84	Full bridge rectifier	10 W
[10]	6.78 MHz	84	Class-E current-driven rectifier	20 W
[11]	13.56 MHz	90.1	Full wave active rectifier	10 mW
[12]	5.56 MHz	90.9	Class-E active rectifier	120 W
This letter	13.56 MHz	94.0%	Passive rectifier	3.2 kW

An important point to notice concerning high-frequency rectifiers is that, most papers that discuss this topic utilize active rectifiers or some sort of additional control to achieve high efficiency [5]–[8], [10]–[13]. Full-bridge rectifiers can also be used. However, their efficiencies are usually lower than their active counterparts [11]. An example of this would be [9], which achieved 84% efficiency.

In this letter, a rectifier which is built using only the passive components is presented. The design has been tested experimentally on a 3.2-kW prototype. The operating frequency is 13.56 MHz and the maximum efficiency is 94.0%. The proposed approach taken in this letter is to first build an accurate simulation model of the circuit, taking into account the parasitic components. To achieve this, PSpice simulator is used. A precise equivalent model of the SiC diode is included in the simulation profile. Next, after the circuit is precisely modeled in simulation, a high-power circuit prototype is optimized to achieve high efficiency. To achieve this, two adjustments have been made: First, a commutation capacitor is added at the input terminals of the rectifier. This capacitor significantly improves the performance of the rectifier by reducing the distortion in input voltage and input current. Second, an inductor is added at the output to transform the output current from discontinuous conduction mode (DCM) to continuous conduction mode (CCM).

### II. HIGH-FREQUENCY HARMONICS AND PARASITIC ELEMENTS

#### A. Parasitic Components

High-frequency rectifiers suffer from severe degradation in their efficiency. Many factors such as diodes forward voltage drop [6], parasitic elements [14], impedance mismatch

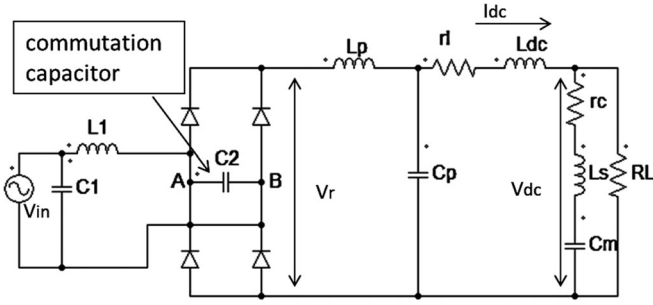


Fig. 1. Equivalent circuit model of high-frequency rectifier including parasitic components (to achieve high efficiency, a commutation capacitor  $C_2$  is added between A and B).

TABLE II

PARAMETERS FOR SIMULATION CIRCUIT (LOW POWER RECTIFIER) OF FIG. 1

$L_1$	$C_1$	$L_p$	$C_p$	$C_m$	$r_c$	$L_s$
0.1 $\mu$ H	10 pF	0.05 $\mu$ H	8 pF	30 nF	0.5 $\Omega$	0.02 $\mu$ H

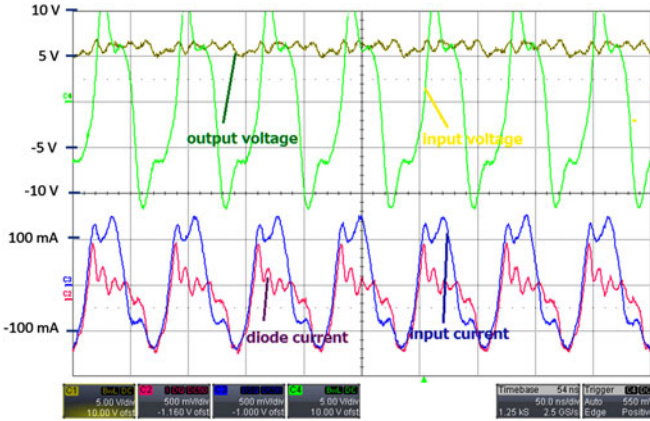


Fig. 2. Waveforms of input voltage, input current, output voltage, and diode current without the commutation capacitor (experiment), load = 100  $\Omega$ , parameters are shown in Table II (time scale = 50 ns/div).

and power reflection [15], and discontinuity in the output current [16] affect the performance of the rectifier. Parasitic inductances and capacitances in the circuit play an important role at high frequencies, causing distortion in the waveforms of the voltages and currents [14].

The simulation model of the high-frequency rectifier, including the parasitic components in the circuit, is shown in Fig. 1.  $L_1$  and  $C_1$  are the inductance and capacitance of the transmission line connecting the source with the rectifier, respectively.  $L_p$  and  $C_p$  are the parasitic inductance and capacitance at the output side of the rectifier, respectively.  $L_{dc}$  is the added dc inductance (see Section III), and  $rl$  is its equivalent series resistance (ESR) (5 m $\Omega$ ).  $C_m$  is the smoothing capacitor,  $r_c$  and  $L_s$  are its ESR and equivalent series inductance (ESI), respectively. Silicon carbide diodes are used for their advantages of faster recovery and low-switching loss [17]. The values of the parameters in Fig. 1 are shown in Table II. The function of the commutation capacitor  $C_2$  as well as the output inductor  $L_{dc}$  will be explained in Section III.

Fig. 2 shows the waveforms of the input voltage, input current, output voltage, and diode current taken from the experiment.

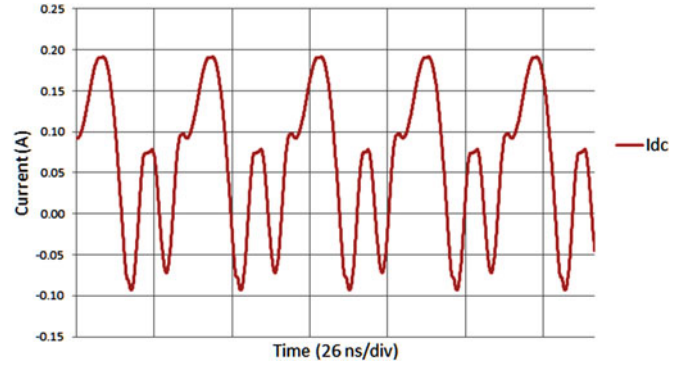


Fig. 3. Simulation results of output current in the discontinuous mode (without commutation capacitor or output inductor), load = 100  $\Omega$ , parameters are shown in Table II.

From the figure, it can be observed that the input voltage and input current are distorted from their normal shapes, also high ripples appear in the diode current.

Another problem that causes reduction in the efficiency of the rectifier is the discontinuity in the output current. When the diode is in the reverse blocking mode, it conducts current for a small period of time which is the recovery time needed to go to the nonconducting state. This results in discharge of the output capacitor through the diode back to the power source. In this period, the output current flows in the reverse direction. This is demonstrated in Fig. 3 in which the output current (see  $I_{dc}$  in Fig. 1) exhibits negative values for some periods of time.

### B. Capacitor's High-Frequency Model

In dc circuits, the model of the capacitor is quite simple: the capacitor is represented by two plates and its capacitance in Farads is given, which is a function of its dimensions and the insulation material used between the plates. However, for high-frequency applications the model is more complicated and involves other parameters, such as the ESR of its leads, which increases as the frequency increases due to the skin effect, and ESI of the leads of the capacitor [18]. Fig. 4 shows the measured impedance of a 10 nF capacitor taken from the network analyzer. The impedance of the capacitor is represented as

$$Z = r_c + j(\omega L_s - 1/(\omega C)) \quad (1)$$

where  $C$  is the capacitance,  $r_c$  is the ESR, and  $L_s$  is the ESI. Referring to Fig. 4(a),  $r_c$  can be measured by taking the lowest value on the curve which corresponds to the resonance frequency of the capacitor (10.5 MHz) at which the impedance is pure resistive and equals to 0.5  $\Omega$ .

Next,  $L_s$  can be calculated based on Fig. 4(b) which shows the phase of the impedance. Below the resonance frequency, the impedance is capacitive (phase =  $-90^\circ$ ), and for frequencies above the resonance the impedance becomes inductive. At the resonance frequency, the capacitive and inductive impedances are equal and therefore  $L_s$  can be calculated as follows:

$$L_s = \frac{1}{\omega_0^2 C} \quad (2)$$

where  $\omega_0$  is the resonant frequency of the capacitor. For this capacitor, the value of  $L_s$  is 0.02  $\mu$ H, as listed in Table II.

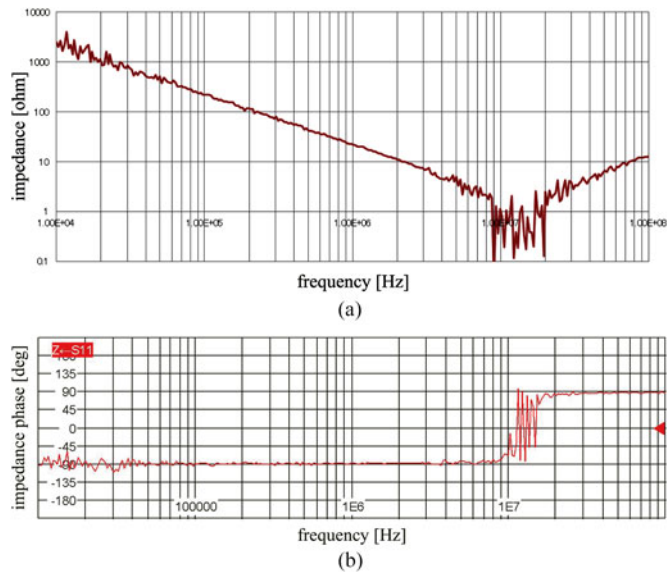


Fig. 4. Impedance of the capacitor: (a) magnitude and (b) phase.

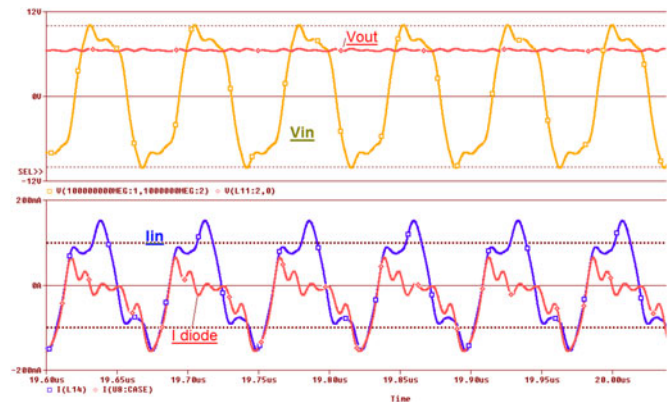


Fig. 5. Waveforms of input voltage, input current, output voltage, and diode current taken from simulation for the circuit in Fig. 1, parameters are shown in Table II.

The parasitic components play a crucial role in wave shaping of the voltages and currents at high frequencies. These parasitic components are responsible for the existence of ripples and distortion in the waves. Fig. 5 shows the input voltage, input current, output voltage, and diode current for the simulation model of the rectifier. Comparing Fig. 5 with Fig. 2, the waveforms are very similar in terms of ripples and distortion.

The next step is to eliminate the high-frequency harmonics to get better wave shapes and higher efficiency.

### III. CIRCUIT MODIFICATION

In this section, we will discuss modifying the shape of the input voltage, as well as the transition of the output current from the discontinuous current mode (DCM) to the continuous current Mode (CCM).

#### A. Commutation Capacitor

Adding a capacitor at the input of the rectifier facilitates the commutation between the diodes when the input voltage

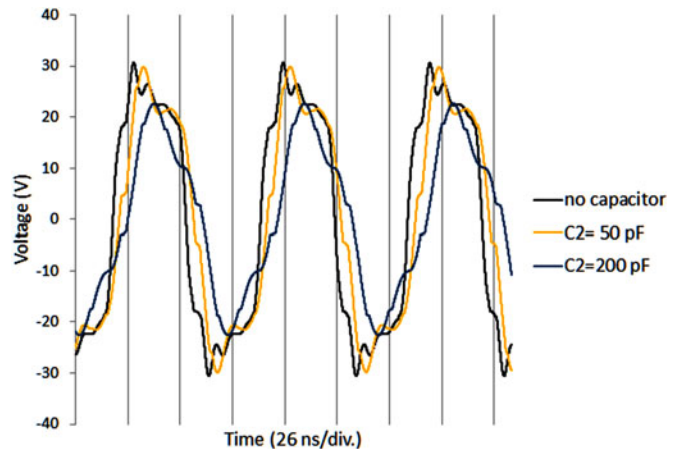


Fig. 6. Effect of different values of commutation capacitor on the input voltage, parameters are shown in Table II, load = 100  $\Omega$ .

switches its polarity. The commutation capacitor (see  $C_2$  in Fig. 1) plays a crucial role in reducing the distortion of the input current and voltage, and also in improving the power factor. It has been shown in Fig. 2 that the input voltage and input current are distorted with high-frequency harmonics. To solve this problem, a commutation capacitor will be added at the input terminals of the rectifier. In Fig. 6, the input voltage is demonstrated for different values of  $C_2$ . It can be concluded that increasing  $C_2$  reduces the harmonics and improves the shape of the input voltage wave. For  $C_2=200$  pF, the input voltage is sinusoidal. It should be noted that albeit  $C_2$  improves the shapes of input voltage and current, it would hinder the performance of the rectifier if it was too large. This is due to the fact that the capacitor's reactance is inversely proportional with its capacitance. Hence, if the capacitance is too large, it would result in the decrease of dc output voltage.

#### B. Output DC Inductance

Adding an inductor in series at the output will force the output current to keep flowing in the same direction. The commutation interval is the time interval at which the two conducting diodes are in the cut-off region and the input voltage switches its polarity preparing for the second half period to start and the other two diodes of the bridge conduct. The energy stored in the inductor should be high enough to prevent the current from falling to zero and switching its direction until the second-half period starts.

Fig. 7 shows the rectified voltage before the filter (see  $V_r$  in Fig. 1), the dc output voltage, and the dc output current for the ideal case. We will assume that the smoothing capacitor  $C_m$  is large enough to keep the output voltage  $V_{dc}$  almost constant. Considering the case that the value of the inductor is such that the output current is at the transition point between the discontinuous and continuous modes, the value of the inductance at this point is the critical inductance  $L_c$ . From the dc side of the rectifier, the following equation is obtained:

$$L_c \frac{di}{dt} = V_{ac} |\sin(\omega t)| - V_{dc}. \quad (3)$$

Since the current in the capacitor in a steady state is zero, the average output current in the inductor equals the load current.

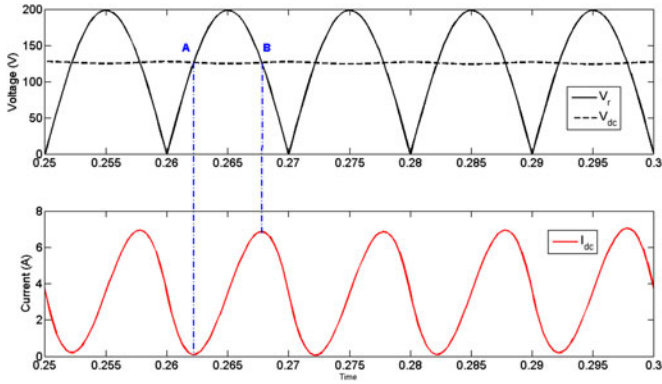


Fig. 7. Output current at critical transition between DCM and CCM.

TABLE III  
SPECIFICATIONS OF RECTIFIER AFTER MODIFICATION

Component	$C_2$	$L_{dc}$	$r_l$	$C_m$	$R_L$
Value	200 pF	10 $\mu$ H	5 m $\Omega$	20 $\mu$ F	10–400 $\Omega$

Consequently, (4) can be derived

$$\frac{\int_0^\pi i_{dc} d\omega t}{\pi} = \frac{V_{dc}}{R_L}. \quad (4)$$

In Fig. 7, the current in the inductor is zero at point A ( $V_r = V_{dc}$ ). The current then increases and reaches its maximum value at point B and decreases again to zero. Solving (3) and (4) at point A, the value of the critical inductance  $L_c$  can be obtained as follows [16]:

$$L_c = \frac{2 \arcsin(\frac{2}{\pi}) + \sqrt{\pi^2 - 4} - \pi}{2\omega} R_L = 0.3307 \frac{R_L}{\omega}. \quad (5)$$

It should be noted that  $L_c$  is the minimum inductance required to make the output dc current just at the boundary between DCM and CCM. Generally, the performance of the rectifier can be improved by increasing the value of the inductance so that the dc current is smooth and almost constant. In the experiment, a 10  $\mu$ H inductor will be used to ensure that the output current remains smooth even under light load or output voltage variations. In Fig. 1,  $L_{dc}$  is the inductor at the dc side of the rectifier, and  $r_l$  is its ESR. For the inductor used in the experiment,  $r_l = 5$  m $\Omega$ .

#### IV. EXPERIMENTS

A high-power source is used to generate the voltage at frequency 13.56 MHz. An impedance matcher is connected between the power source and the rectifier to reduce the reflected power [15]. The rated power of the rectifier is 3.2 kW. Silicon carbide Schottky diodes of 20 A rated current are used (C2D20120D) for their small recovery time. Table III demonstrates the components used in the high-power rectifier and their values. Two parallel, 100 pF, ceramic capacitors are used in the experiment. Fig. 8 shows the experimental prototype of the rectifier.

In Fig. 9, the waveforms of the input voltage, rectified voltage ( $V_r$  in Fig. 1), output voltage, and output current are demonstrated. The figure shows that the output current is continuous and constant, some distortion appears in the wave of

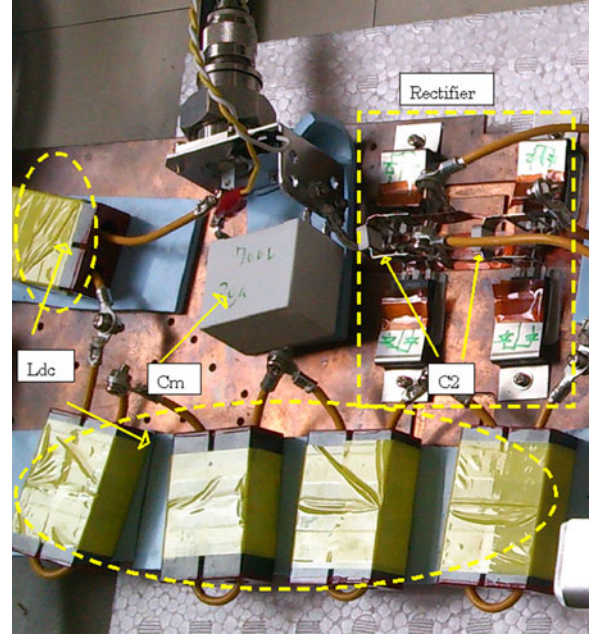


Fig. 8. Experimental prototype of high-frequency rectifier.

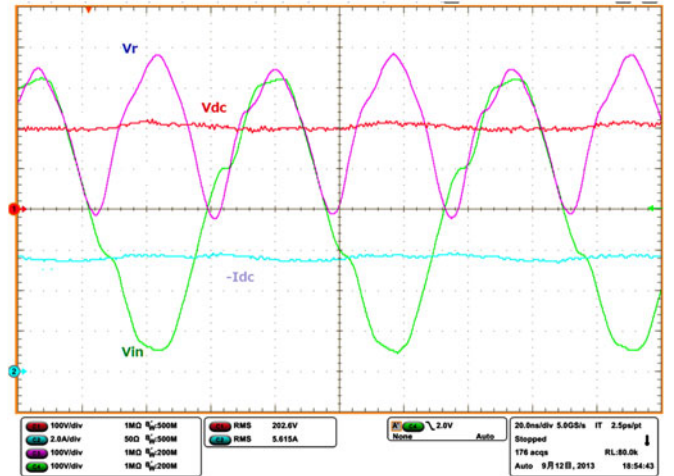


Fig. 9. Waveforms of input voltage, rectified voltage, dc voltage, and dc current after adding commutation capacitor and output inductor, parameters are shown in Table III (experiment).

the input voltage, but has been significantly reduced compared to that in Fig. 2.

In Table IV, the input power is increased from 143.6 to 3310 W while the output voltage is fixed at 200 V. The table shows the efficiency for each case. Notice that the efficiency is dependent upon the input power. Increasing the input power increases the efficiency of the rectifier with highest efficiency of 94.0%. The same result is depicted in Fig. 10. The interpretation of the power-efficiency pattern obtained in Fig. 10 is as follows: Under light-load condition, the output current is relatively small. Hence, the energy stored in the output inductor is small and the output current is in the DCM. Under heavy load condition, the output current increases, and so does the stored energy. Hence, the inductor has enough energy to keep the current flowing in the same direction until the second-half cycle begins. This

TABLE IV  
MEASUREMENT OF EFFICIENCY FOR VARIABLE INPUT POWER  
AND FIXED OUTPUT VOLTAGE

$P_{in}$ (W)	$P_r$ (W)	$V_{dc}$ (V)	$I_{dc}$ (A)	$P_{out}$ (W)	Efficiency (%)
143.6	0.67	198	0.55	108.9	76.19
377	0.33	200	1.65	330	87.61
490	0.44	199.8	2.2	439.6	89.79
1174	0.30	199.5	5.5	1097.3	93.49
1679	0.35	199.5	7.85	1566.1	93.29
2340	0.35	198	11.1	2197.8	93.94
2850	0.16	199.8	13.4	2677.3	93.95
3310	0.64	199.5	15.6	3112.2	94.04

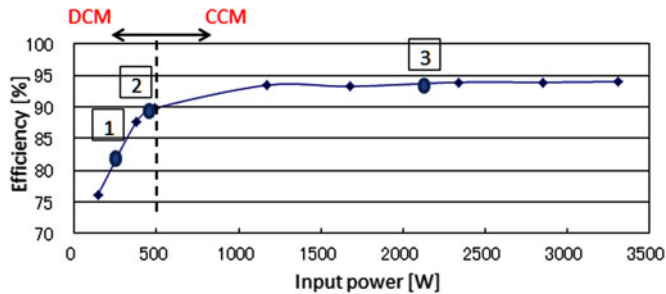


Fig. 10. Rectifier input power versus efficiency for different load conditions and fixed output voltage = 200 V (experiment).

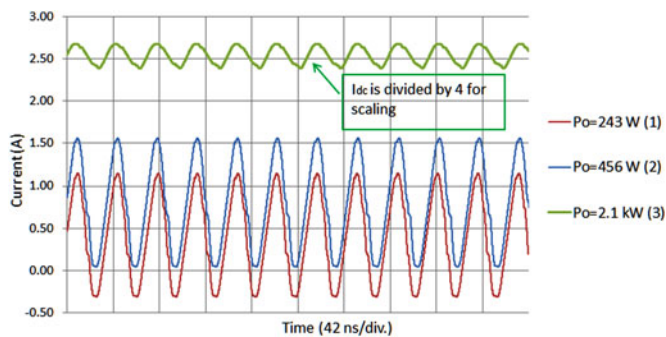


Fig. 11. Simulation results of  $I_{dc}$  for different load conditions, parameters of the rectifier are as in Table III, input voltage = 1000 V. The three points (1, 2, and 3) are marked on Fig. 10.

conclusion can be observed in Fig. 11, which shows  $I_{dc}$  for different power conditions (245, 456, and 2.1 kW). The figure shows that for low power,  $I_{dc}$  is in DCM. At load condition 2 (456 W),  $I_{dc}$  is at the transition state, and for power = 2.1 kW the current is already in CCM. The three points in Fig. 11 are marked in Fig. 10. For low-power condition, to make the current flow in CCM,  $L_{dc}$  should be increased, as confirmed by (5).

## V. CONCLUSION

This paper presented a high-efficiency ac/dc passive rectifier with a commutation capacitor for the high-frequency applications. It has been shown that the parasitic elements in the circuit generate high-frequency harmonics. A commutation capacitor is added at the input of the rectifier to improve the power factor and reduce the attenuation in the voltage. Due to the high frequency of the source, the output current is in the DCM which causes reduction in the efficiency of the rectifier and the overall system. The output current can be transformed into the CCM by adjust-

ing the output inductance. The advantages of the rectifier are its high efficiency and simplicity compared to active rectifiers.

## REFERENCES

- [1] J. Yin, D. Lin, C.-K. Lee, and S. Y. R. Hui, "A systematic approach for load monitoring and power control in wireless power transfer systems without any direct output measurement," *IEEE Trans. Power Electron.*, vol. 30, no. 3, pp. 1657–1667, Mar. 2015.
- [2] W. Zhong and S. Y. R. Hui, "Auxiliary circuits for power flow control in multifrequency wireless power transfer systems with multiple receivers," *IEEE Trans. Power Electron.*, vol. 30, no. 10, pp. 5902–5910, Oct. 2015.
- [3] M. B. Shamsheh, A. Kawamura, I. Yuzurihara, and A. Takayanagi, "A wireless power transfer system optimized for high efficiency and high power applications," in *Proc. Int. Power Electron. Conf.*, pp. 2794–2801, 2014.
- [4] N. K. Trung, T. Ogata, S. Tanaka, and K. Akatsu, "Analysis and PCB design of class D inverter for wireless power transfer systems operating at 13.56 MHz," *IEEJ J. Ind. Appl.*, vol. 6, no. 6, pp. 703–713, 2015.
- [5] E. Asa, K. Colak, M. Bojarski, and D. Czarkowski, "A novel phase control of semi bridgeless active rectifier for wireless power transfer applications," in *Proc. IEEE Appl. Power Electron. Conf. Expo.*, pp. 3225–3231, 2015.
- [6] S. Aldhaher, P. C.-K. Luk, K. El Khamlichi Drissi, and J. F. Whidborne, "High-input-voltage high-frequency class E rectifiers for resonant inductive links," *IEEE Trans. Power Electron.*, vol. 30, no. 3, pp. 1328–1335, Mar. 2015.
- [7] W. Zhu, K. Zhou, M. Cheng, and F. Peng, "A high-frequency-link single-phase PWM rectifier," *IEEE Trans. Ind. Electron.*, vol. 61, no. 1, pp. 289–298, Jan. 2015.
- [8] H. Park, J. Jang, H. Kim, Y. Park, S. Oh, Y. Park, K. Hwang, Y. Yang, and K. Lee, "A design of a wireless power receiving unit with high efficiency 6.78 MHz active rectifier using shared DLLs for magnetic resonant A4WP applications," *IEEE Trans. Power Electron.*, vol. 31, no. 6, pp. 4484–4498, Jun. 2015.
- [9] M. Fu, Z. Tang, M. Liu, C. Ma, and X. Zhu, "Full-bridge rectifier input reactance compensation in megahertz wireless power transfer systems," in *Proc. IEEE PELS Workshop Emerg. Technol.: Wireless Power*, vol. 31, no. 6, pp. 4280–4291, 2016.
- [10] M. Liu, M. Fu, and C. Ma, "Parameter design for a 6.78-MHz wireless power transfer system based on analytical derivation of class E current-driven rectifier," *IEEE Trans. Power Electron.*, vol. 31, no. 6, pp. 1–5, Jun. 2015.
- [11] Y. Lu and W.-H. Ki, "A 13.56 MHz CMOS active rectifier with switched-offset and compensated biasing for biomedical wireless power transfer systems," *IEEE Trans. Biomed. Circuits Syst.*, vol. 8, no. 3, pp. 334–344, Jun. 2014.
- [12] G. Kkelis, J. Lawson, D. C. Yates, M. Pinuela, and P. D. Mitcheson, "Integration of a class-E low DV/DT rectifier in a wireless power transfer system," in *Proc. IEEE Wireless Power Transfer Conf.*, pp. 72–75, 2014.
- [13] B. Veerasamy, W. Kitagawa, and T. Takeshita, "Output ripple minimization of single-stage power-factor-correction bidirectional buck AC/DC converter," *IEEJ J. Ind. Appl.*, vol. 4, no. 3, pp. 235–243, 2015.
- [14] Y. Du, G. Wang, J. Wang, and S. Bhattacharya, "Modeling of the impact of diode junction capacitance on high voltage high frequency rectifiers based on 10 kV SiC JBS diodes," in *Proc. IEEE Energy Convers. Congr. Expo.*, pp. 105–111, 2010.
- [15] K. Kusaka and J. Itoh, "Input impedance matched AC–DC converter in wireless power transfer for EV charger," in *Proc. Int. Conf. Electr. Mach. Syst.*, pp. 1–6, 2012.
- [16] P. Si and A. P. Hu, "Analyses of DC inductance used in ICPT power pickups for maximum power transfer," in *Proc. IEEE PES Transmiss. Distrib. Conf. Exhib.*, pp. 1–6, 2005.
- [17] K. Kusaka and J. Itoh, "Experimental verification of rectifiers with SiC/GaN for wireless power transfer using a magnetic resonance coupling," in *Proc. IEEE Int. Conf. Power Electron. Drive Syst.*, pp. 1094–1099, 2011.
- [18] S. Siami, C. Joubert, and C. Glaize, "High frequency model for power electronics capacitors," *IEEE Trans. Power Electron.*, vol. 16, no. 2, pp. 157–166, Mar. 2001.